Three-dimensional properties of Andes mountain waves observed by satellite: A case study

M. Joan Alexander[1] and Hector Teitelbaum[2]

Received 25 April 2011; revised 26 September 2011; accepted 26 September 2011; published 10 December 2011.

[1] The southern Andes region has been clearly identified in previous satellite and balloon observations and in global models as a "hot spot" of small-scale gravity wave activity, with monthly mean momentum fluxes exceeding 10 times background values in fall, winter, and spring seasons. This makes this region a focus of interest for global circulation and climate studies. We analyze a case study on 8 May 2006, combining observations from the Atmospheric Infrared Sounder instrument on the Aqua satellite and the High Resolution Dynamics Limb Sounder instrument of the Aura satellite to form a three-dimensional picture of the wave field. The observations show a widespread wave pattern over the southern Andes extending eastward over the south Atlantic. Simulations with the Weather Research Forecasting model clearly identify the waves as orographic in origin, but the observed wave pattern is far from the simple two-dimensional wave field forced by steady flow over a mountain ridge. The morphology of the pattern is consistent with three-dimensional linear theoretical calculations of downstream propagation and latitudinal focusing of mountain waves into the stratospheric jet. The observations confirm the importance of this process in the stratosphere, and we find the process also occurring in the global analysis and forecasts from the European Centre for Medium-Range Weather Forecasting. Our analysis evaluates some strengths and weaknesses of current orographic wave drag parameterizations in global models and the relevance of parameterization assumptions in global models with high resolution.

Citation: Alexander, M. J., and H. Teitelbaum (2011) Three-dimensional properties of Andes mountain waves observed by satellite: A case study, *J. Geophys. Res.*, *116*, D23110, doi:10.1029/2011JD016151.

1. Introduction

[2] Chemical and dynamical processes in the Southern Hemisphere stratosphere have well known effects on the development of the ozone hole and its predicted recovery in the 21st century. Recent research has also uncovered a relationship between stratospheric ozone recovery and projected changes in the seasonal cycle of surface winds in the Southern Hemisphere [*Perlwitz et al.*, 2008; *Son et al.*, 2008; *Turner et al.*, 2009]. Gravity wave drag in the high-latitude winter season stratosphere has a strong effect on the strength of vortex winds, vortex temperatures, and the depth and timing of the development of the ozone hole each year [e.g., *Austin and Wilson*, 2006; *Schmidt et al.*, 2006; *Alexander et al.*, 2010].

[3] As early as 1996, space-based methods for detecting small-scale temperature fluctuations in the stratosphere identified the region over the southern Andes as a hot spot of small-scale wave activity [*Wu and Waters*, 1996; *Jiang et al.*, 2002; *Eckermann and Preusse*, 1999; *Wu and Eckermann*, 2008; *Wells et al.*, 2011]. More recently, methods for estimating gravity wave momentum flux globally also identified this region as an important source for waves contributing to drag on the Southern Hemisphere winds [*Ern et al.*, 2004; *Alexander et al.*, 2008; *Hertzog et al.*, 2008], confirming earlier model results [*Bacmeister*, 1993].

[4] This paper describes an in depth case study of gravity waves in the stratosphere over the Southern Andes in this hot spot region. We present the three-dimensional structure of the wave field as observed from two satellite instruments: the Atmospheric Infrared Sounder (AIRS) instrument on the Aqua satellite and the High Resolution Dynamics Limb Sounder (HIRDLS) instrument on the Aura satellite. The case, on 8 May 2006, displays a morphology with short horizontal wavelength waves directly above and approximately aligned with the Andes ridge and longer horizontal wavelength waves downstream, with phase fronts aligned northwest to southeast.

[5] A previous study using coarser-resolution satellite measurements observed some features of a similar downstream field and identified a southeastward group velocity for mountain waves in this region [*Preusse et al.*, 2002]. More recently, similar downstream propagation with focusing into the stratospheric jet was identified in a global gravity wave resolving model study [*Sato et al.*, 2011]. The downstream wave propagation was described with a three-dimensional

[1]NorthWest Research Associates, Boulder, Colorado, USA.
[2]Laboratoire de Meteorologie Dynamique, Paris, France.

0148-0227/11/2011JD016151

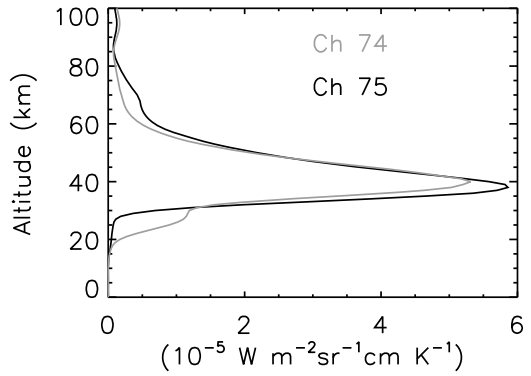

Figure 1. Temperature kernels for AIRS channels 74 and 75. The measured radiance at these channels is due to emissions from stratospheric altitudes, with the kernels peaking at 40 and 38 km, respectively.

linear, small-amplitude theory for mountain wave propagation. The southward and downstream propagation described in this *Sato et al.* [2011] study results when a component of the wave propagation vector is perpendicular to the wind vector. (Note the global model in the *Sato et al.* [2011] study did not resolve the shorter horizontal wavelength features we observe with AIRS directly above the Andes.)

[6] Here we compare the AIRS and HIRDLS satellite measurements to Weather Research Forecasting (WRF) model simulations of the 8 May 2006 case, and the comparison provides a validation of the gravity waves in the model. Close examination of the model further reveals nonlinearities in the wave field in the stratosphere that suggest some alteration of the simpler picture afforded by the linear theory. An analysis of the satellite data gives a measure of spatial variations of momentum flux across the wave pattern, and we contrast wave properties directly above the topography with those downstream. We also compare to the operational atmospheric data from the European Centre for Medium-Range Weather Forecasting (ECMWF), which in 2006 was provided at a resolution of T799 with 91 vertical levels. The results permit an observationally based case study estimation of the relative roles of smaller-scale parameterized and resolved waves that would be appropriate in a high-resolution global model.

2. Description of the Satellite Observations

[7] The AIRS instrument on the Aqua satellite and the HIRDLS instrument on Aura fly in formation in the international "A-Train" satellite constellation [*Schoeberl et al.*, 2004]. The A-Train satellites fly at high-inclination, with equatorial crossings at fixed local solar times of 1:30 am and 1:30 pm. Although the orbit tracks for AIRS-Aqua and HIRDLS-Aura are coincident, AIRS is a cross-track nadir scanning instrument while HIRDLS is a limb scanner with a line of sight azimuth angle of 47° to the anti-Sun side of the orbital plane [*Gille et al.*, 2008]. Thus instead of viewing the same geographical region nearly simultaneously with other A-Train instruments, the same location is viewed on a preceding or following orbit.

[8] AIRS observations of the southern Andes region on 8 May 2006 occur at approximately 05:45 UT and 19:15 UT. HIRDLS views the same location at approximately 03:00 UT and 21:15 UT. Since mountain waves are approximately stationary and develop on timescales of hours to days, we neglect these minor differences in timing, but retain the AM/PM distinction. We will subsequently refer to these two events as 05:00 UT and 20:00 UT for the AM and PM observations, respectively. The AM/PM distinction will be shown to be important primarily because of differences in the HIRDLS viewing geometry in these two cases.

[9] For AIRS, we use radiance imagery of the 8 May event using two channels in the 15-μm emission band from CO_2 that peak in the stratosphere: Channels 74 (667.5 cm^{-1}) and 75 (667.8 cm^{-1}). Figure 1 shows the kernel functions for these channels for polar winter conditions [*Hoffmann and Alexander*, 2009]. The peaks lie at ~40 and 38 km, respectively. Radiance anomalies are computed as deviations from a fourth-order polynomial fit in the cross-track directions which effectively removes the scan angle dependence in the radiances. The background removal effectively filters waves with horizontal wavelengths longer than ~500 km. Brightness temperature anomalies are computed from radiance anomalies as described by *Alexander and Barnet* [2007] using a background temperature $\bar{T}$ = 235 K. AIRS observations give a horizontal plan view of brightness temperature perturbations over the region with a 13.5-km diameter horizontal footprint at the nadir, and an average footprint of ~20 km diameter. The imagery represent an integrated measurement in height, as described by the kernel functions in Figure 1, which would effectively eliminate any short vertical wavelength waves. The fast eastward wind speeds in the stratosphere lead to refraction of the mountain waves to long vertical wavelengths that can survive this vertical integration.

[10] HIRDLS, conversely, gives cross sections of temperature perturbation with fine vertical resolution. The instrument field of view projected onto the limb has a vertical width of 1.2 km, and the HIRDLS temperature retrievals can effectively resolve waves with vertical wavelengths as short as 4 km [*Alexander and Ortland*, 2010]. The horizontal resolution along the measurement track is determined by the spacing between vertical profiles, which is ~100 km. Along the line of sight, the limb measurement represents an integral with the typical horizontal length of ~150 km. Short horizontal wavelength waves with phase fronts perpendicular to the line of sight will therefore be effectively filtered from the HIRDLS measurements, while if their phase fronts are parallel to the line of sight they can be observed, but undersampled [e.g., *Eckermann and Preusse*, 1999].

[11] HIRDLS gravity wave perturbations are computed here as temperature anomalies from the large scale. The large scale is defined as the zonal mean plus planetary scale waves with zonal wave numbers 1–3 [*Alexander et al.*, 2008].

3. WRF Model Description

[12] Weather Research Forecasting model (WRF [*Skamarock et al.*, 2005]) simulations are configured to investigate whether the waves seen in the satellite data are orographic waves. WRF is run in a nested configuration covering the Southern Andes region. An outer domain has horizontal resolution 21-km and 2000 × 2000 km^2 area, and an inner domain with 7-km resolution and 700 × 700 km^2

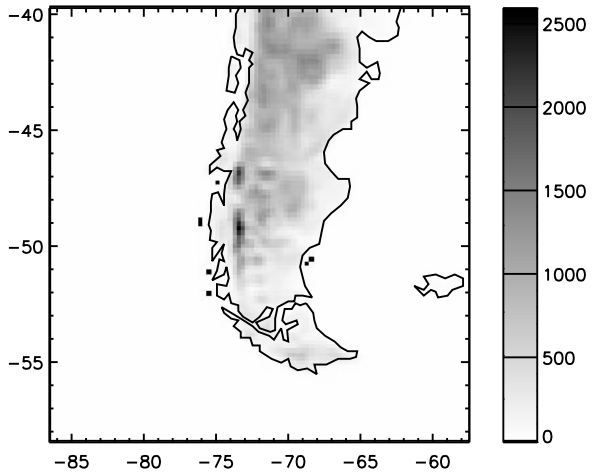

Figure 2. Topography (m) of the southern Andes mountains shown at resolution of the outer WRF model domain.

area over the Andes topography is centered within. The model extends from the surface to 45 km in the vertical with 115 levels. We include a sponge layer above 40 km to limit wave reflection from the top boundary. Vertical resolution increases from 0.2 km at low levels to 0.6 km at 30 km altitude, then further increases to 2 km in the sponge layer. The model is initialized at 00:00 UT on 7 May with ECMWF analysis fields and the analysis defines conditions at the outer boundaries of the large domain throughout the simulation. We also initiated another run at 00:00 UT on 8 May to examine any influence of incomplete absorption in the sponge layer on the solutions. This comparison shows some wave reflection from the top boundary appearing as weak perturbations on the observed wave pattern, although the slower, longer waves in the field do not have sufficient time to fully develop at the satellite observation level in this case, so we do not examine this simulation further.

[13] Topography on the 21-km domain grid is shown in Figure 2. The zonal wind upstream of the topography is shown in Figure 3. Low-level upstream winds are southeastward with speeds up to 30 m s^{-1} and peaking at latitudes with the highest terrain. Winds in the stratosphere are primarily zonal and reach 55 m s^{-1} near 40 km altitude. Within the model domain (40–60°S), the jet in the stratosphere increases gradually with increasing southern latitude. The model includes microphysics using the Thompson scheme [*Thompson et al.*, 2004], but moist processes are rather unimportant in this case study. Only very light rain occurs along the coast west of the mountains, accumulations less than 2.5 mm in the 4 h from 0 to 04:00 UT on 8 May. These are small values that are unlikely to be involved in wave forcing in any significant way. A second simulation with the same configuration, except without the mountains, is also performed for comparison.

4. Model Comparison to Observations

[14] The AIRS channel brightness temperature anomalies (T_B') for the AM (05:00 UT) and PM (20:00 UT) overpasses are shown in Figure 4, as the average of channels 74 and 75. Only perturbations with $|T_B'| > 0.4$K, which is 3 times the estimated noise, are colored. These are otherwise raw, unsmoothed, unfiltered data. Bands of alternating positive and negative T_B' can be seen running roughly parallel to the west coastal outline and downstream between ~45° and 50°S latitude, and further north to 40°S in the PM case. These features have short horizontal wavelengths <100 km, approaching the AIRS resolution limits. Extending from these to the south and east are longer horizontal wavelength features, which extend out over the sea well beyond any topography. These qualitatively resemble the topographic waves observed to propagate downstream and southward, focusing in the stratospheric jet to the south and east of the Andes topography, in the global simulations reported by *Sato et al.* [2011]. The wave field is observed to be approximately stationary during the 15 h interval separating the AM and PM overpasses.

[15] Figure 5 shows temperatures at 40 km altitude in the WRF simulation at 05:00 UT and 20:00 UT for comparison to the AIRS observations. The observed wave pattern is well reproduced in the simulation, including the pattern location, wave orientation, and horizontal wavelengths. The largest amplitude shorter horizontal wavelength waves are observed parallel to and in the lee of the main Andes ridge. Weaker longer horizontal wavelength waves are also observed to extend to the south and east over the south Atlantic Ocean with similar orientation as those in the observations. Locations of HIRDLS profiles along the HIRDLS measurement track are overplotted on these maps with black circles.

[16] Figure 6 shows profiles of the HIRDLS gravity wave temperature anomalies arranged in sequence to show a longitude-height cross section along the line formed by the measurement track for both the AM (05:00 UT) and PM (20:00 UT) overpasses. For comparison, Figure 7 shows vertical cross sections of the model sampled along the HIRDLS measurement track. Model temperatures here are shown as perturbations from the trend along the section computed at each altitude. Comparison of Figures 6 and 7 show close quantitative agreement between the gravity

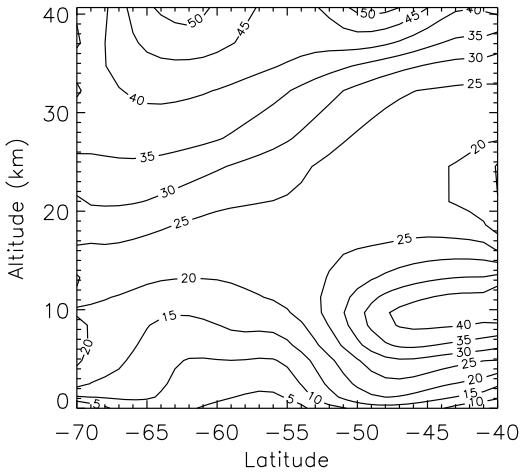

Figure 3. Upstream zonal wind (contours every 5 m s^{-1}), averaged between 80 and 100° W longitude, on 8 May versus latitude and height from the 06:00 UT ECMWF analysis. Eastward surface winds maximize between 45 and 50°S and stratospheric vortex winds exceed 50 m s^{-1} between 60 and 65°S.